

Supporting Information

# Elemental Selenium Enables Enhanced Water Oxidation Electrocatalysis of NiFe Layered Double Hydroxides

Shuo Duan,<sup>a</sup> Shaoqing Chen,<sup>b</sup> Tanyuan Wang,<sup>a,\*</sup> Shenzhou Li,<sup>a</sup> Jianyun Liu,<sup>a</sup> Jiashun Liang,<sup>a</sup> Haiqin Xie,<sup>a</sup> Jiantao Han,<sup>a</sup> Shuhong Jiao,<sup>c</sup> Ruigo Cao,<sup>c</sup> Hsing-Lin Wang,<sup>b</sup> Qing Li<sup>a,\*</sup>

<sup>a</sup>State Key Laboratory of Material Processing and Die & Mould Technology, School of Materials Science and Engineering, Huazhong University of Science and Technology, Wuhan, Hubei 430074, China

<sup>b</sup>Department of Materials Science and Engineering, Southern University of Science and Technology, Shenzhen, Guangdong 518055, China

<sup>c</sup>Key Laboratory of Materials for Energy Conversion Chinese Academy of Science (CAS), Department of Materials Science and Engineering, University of Science and Technology of China, Hefei 230026, China

\*Corresponding Authors. E-mails: [qing\\_li@hust.edu.cn](mailto:qing_li@hust.edu.cn) (Q. Li); [wangty@hust.edu.cn](mailto:wangty@hust.edu.cn) (T. Wang).

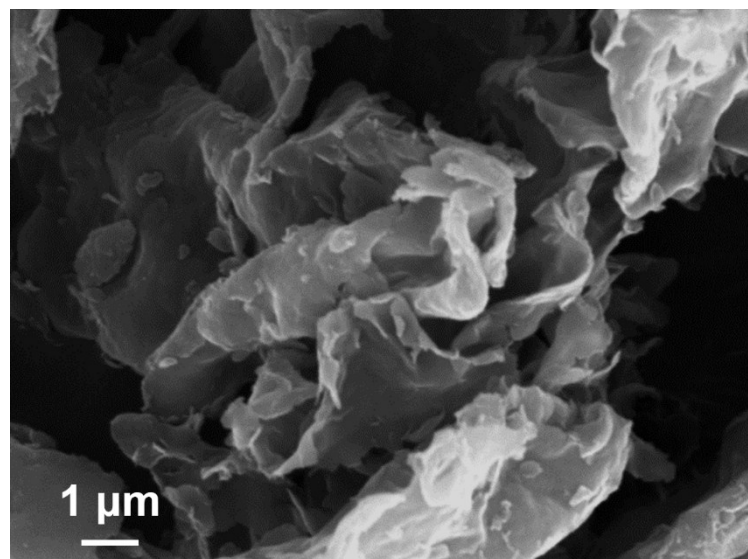


**Figure S1.** SEM image of Ni<sub>0.8</sub>Fe<sub>0.2</sub>-LDH.

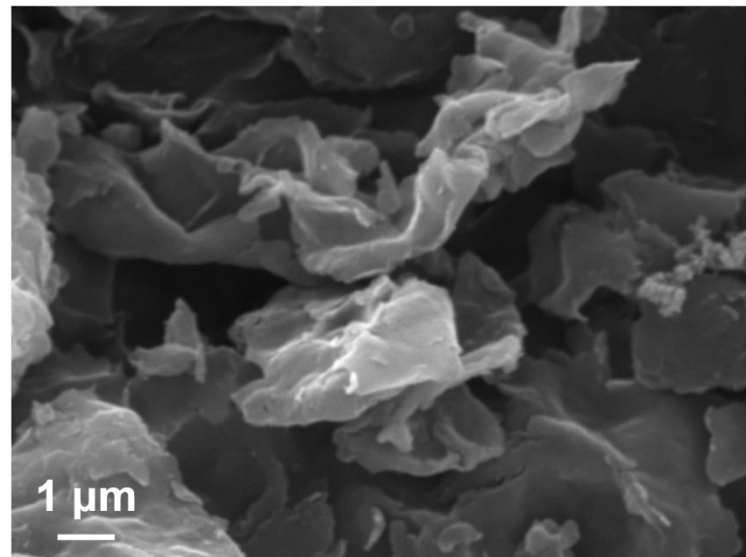


**Figure S2.** SEM image of Ni<sub>0.8</sub>Fe<sub>0.2</sub>-t-Se<sub>0.02</sub>-LDH.

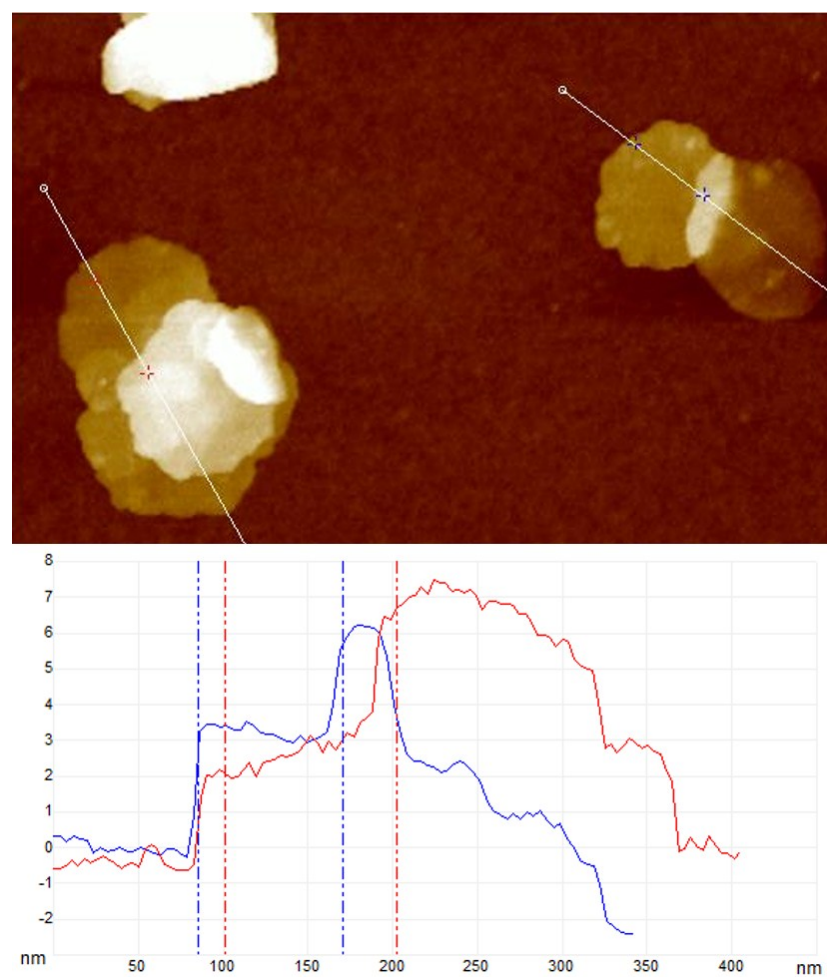


**Figure S3.** AFM image of  $\text{Ni}_{0.8}\text{Fe}_{0.2}\text{-t-}\text{Se}_{0.02}\text{-LDH}$ .

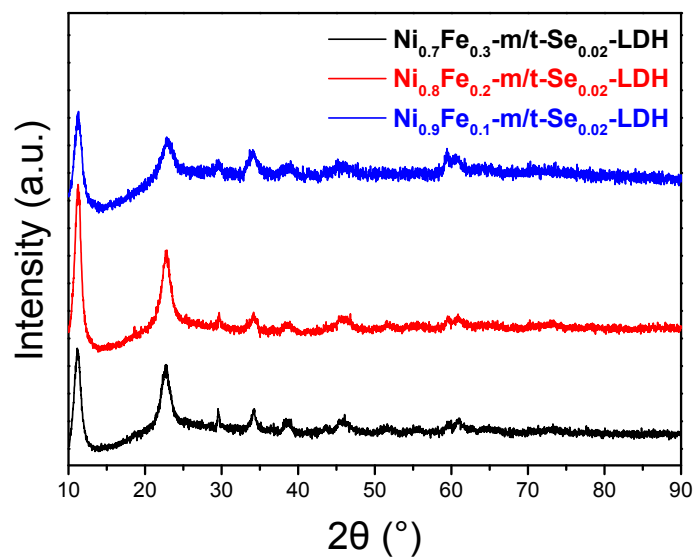


**Figure S4.** XRD patterns of NiFe-m/t-Se-LDH with different Ni/Fe ratios.

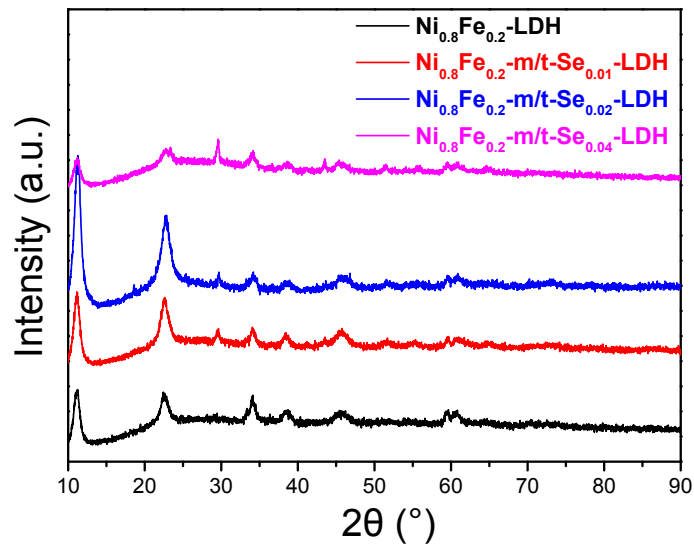


**Figure S5.** XRD patterns of  $\text{Ni}_{0.8}\text{Fe}_{0.2}\text{-m/t-Se-LDH}$  with different doping amounts of m/t-Se.

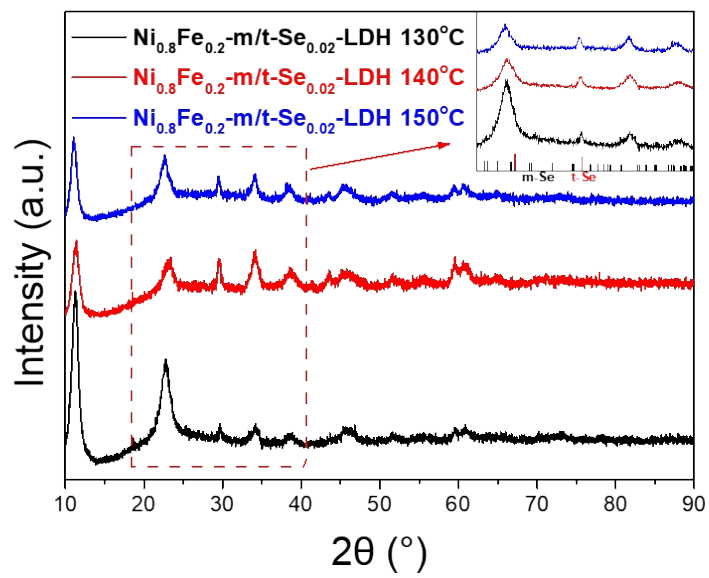


**Figure S6.** XRD patterns of  $\text{Ni}_{0.8}\text{Fe}_{0.2}\text{-m/t-Se}_{0.02}\text{-LDH}$  with different hydrothermal temperatures at  $130^\circ\text{C}$ ,  $140^\circ\text{C}$  and  $150^\circ\text{C}$ ; insert figure: Partial enlarged XRD patterns of  $\text{Ni}_{0.8}\text{Fe}_{0.2}\text{-m/t-Se}_{0.02}\text{-LDH}$  with different hydrothermal temperatures.

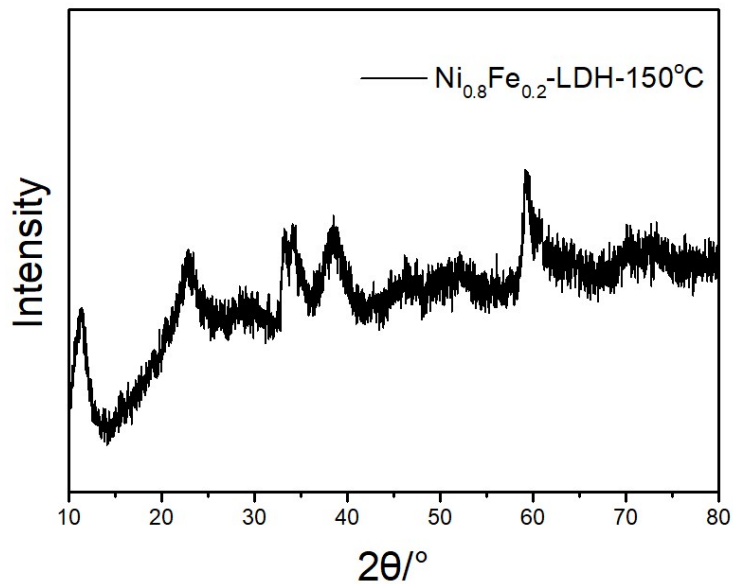


**Figure S7.** XRD pattern of  $\text{Ni}_{0.8}\text{Fe}_{0.2}\text{-LDH}$  with the hydrothermal temperature of  $150^\circ\text{C}$ .

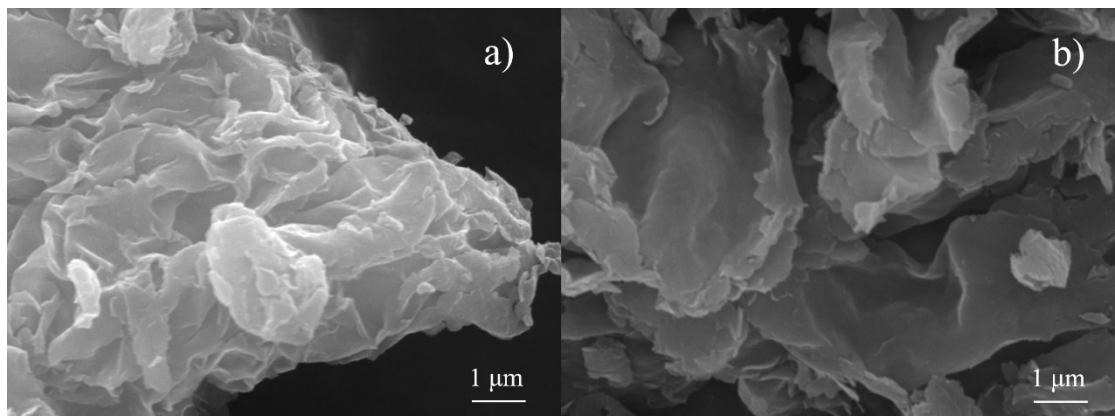


**Figure S8.** SEM images of (a) Ni<sub>0.8</sub>Fe<sub>0.2</sub>-LDH and (b) Ni<sub>0.8</sub>Fe<sub>0.2</sub>-m/t-Se<sub>0.02</sub>-LDH with the hydrothermal temperature of 150 °C.

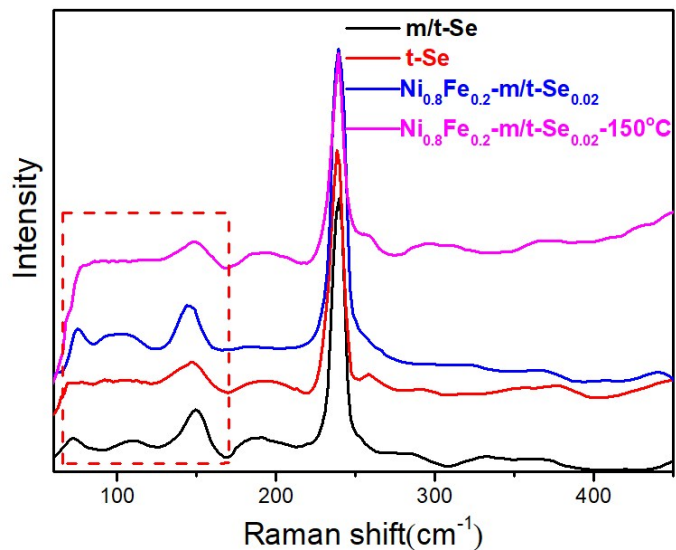


**Figure S9.** Raman spectra of m/t-Se(black line), t-Se(red line), Ni<sub>0.8</sub>Fe<sub>0.2</sub>-m/t-Se<sub>0.02</sub>-LDH(blue line) and Ni<sub>0.8</sub>Fe<sub>0.2</sub>-t-Se<sub>0.02</sub>-LDH(pink line).

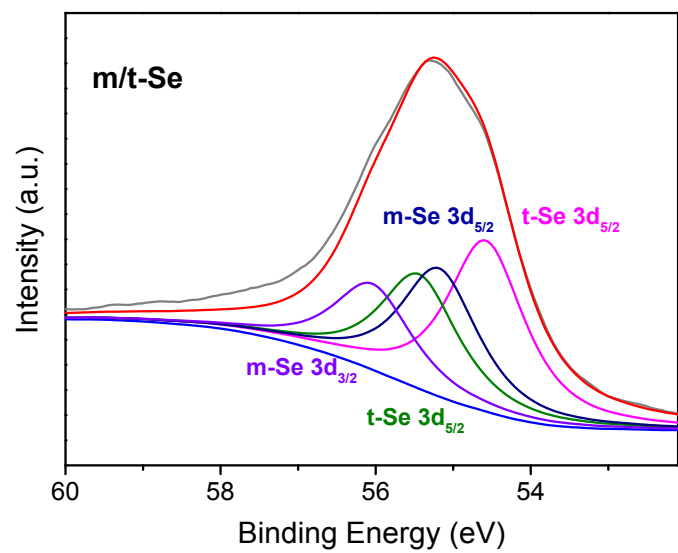


**Figure S10.** High-resolution Se 3d XPS spectrum of m/t-Se.

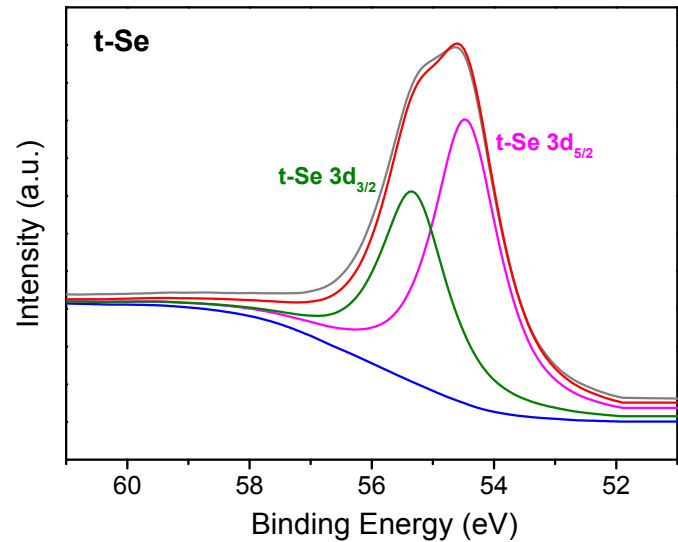


**Figure S11.** High-resolution Se 3d XPS spectrum of t-Se.

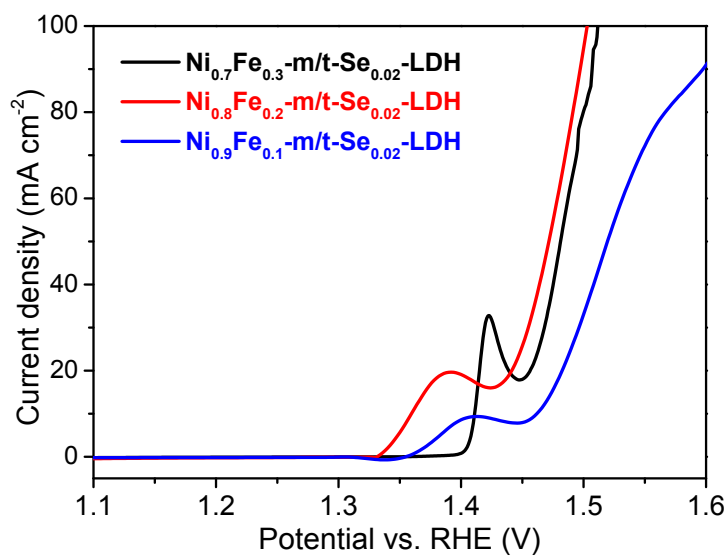


**Figure S12.** OER polarization curves of NiFe-m/t-Se-LDH catalysts with different Ni/Fe ratios.

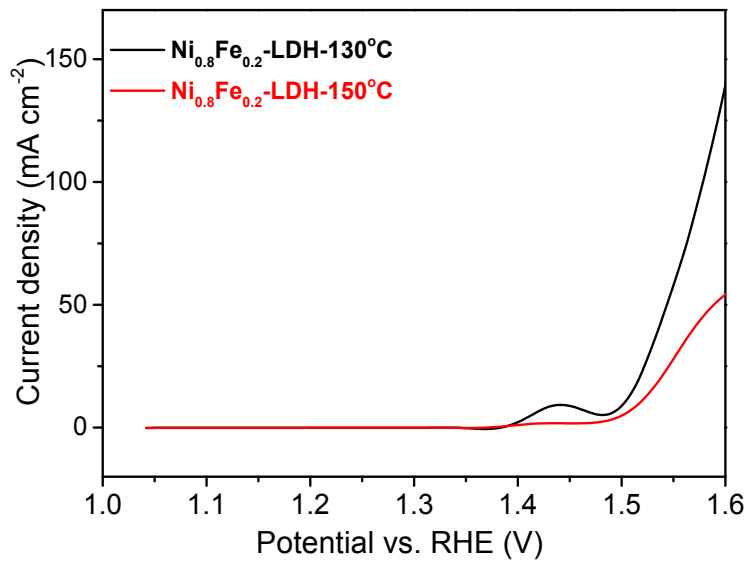


**Figure S13.** OER polarization curves of NiFe-LDH catalysts with different synthesis temperatures.

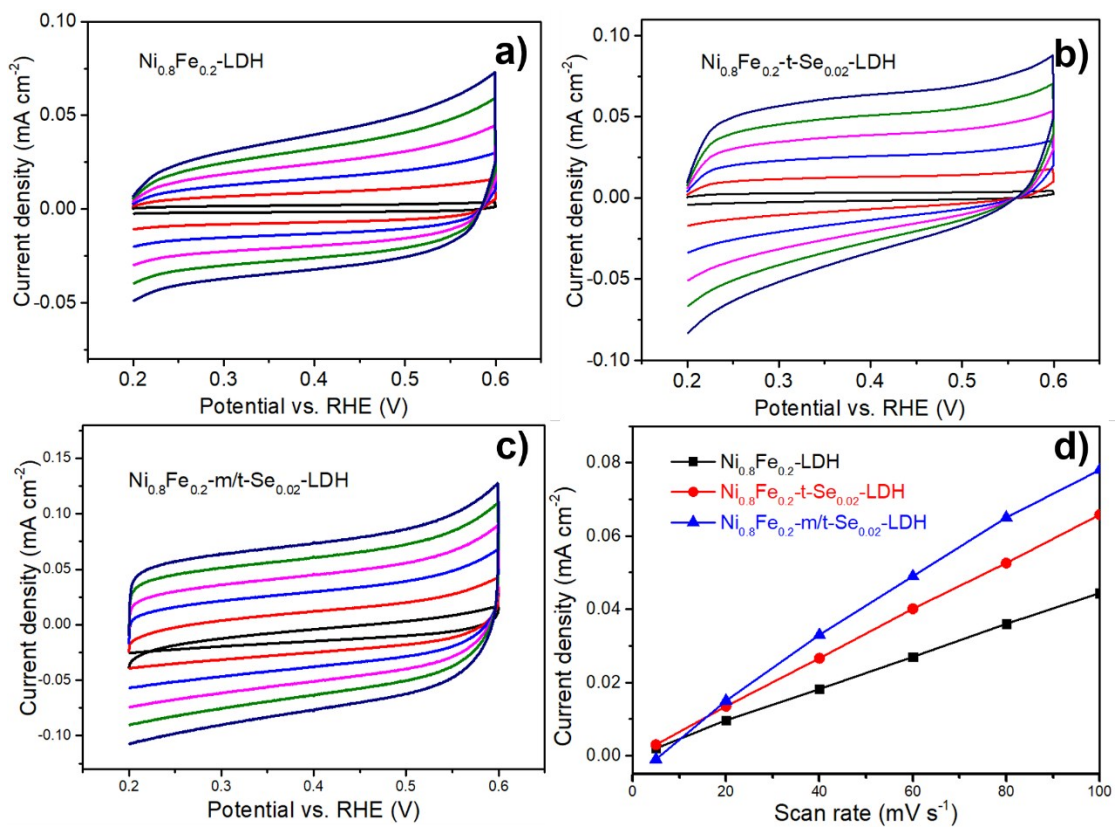


**Figure S14.** Non-Faradaic cyclic voltammograms of (a) Ni<sub>0.8</sub>Fe<sub>0.2</sub>-Se<sub>0.02</sub>-LDH, (b) Ni<sub>0.8</sub>Fe<sub>0.2</sub>-m/t-Se<sub>0.02</sub>-LDH, and (c) Ni<sub>0.8</sub>Fe<sub>0.2</sub>-m/t-Se<sub>0.02</sub>-LDH in 1.0 M KOH electrolyte at scan rate of 5, 20, 40, 60, 80, and 100 mV/s. (d) Anodic and cathodic current densities at 0.45 V versus the scan rate.

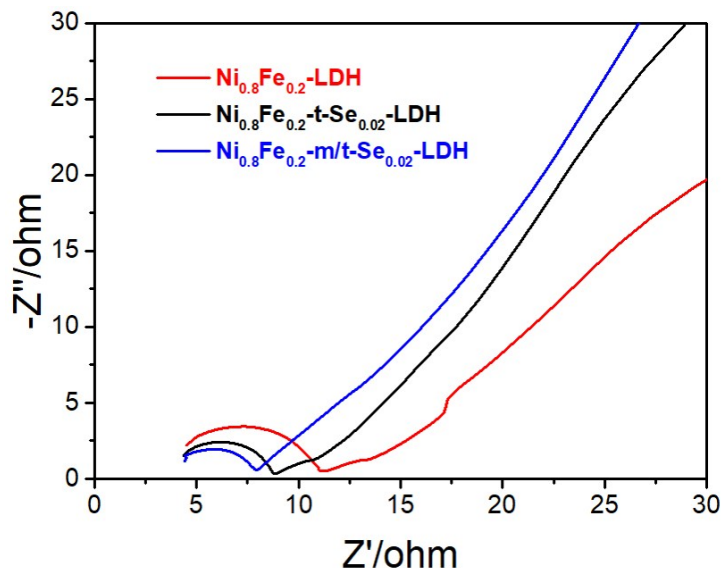


**Figure S15.** EIS plots of Ni<sub>0.8</sub>Fe<sub>0.2</sub>-LDH, Ni<sub>0.8</sub>Fe<sub>0.2</sub>-t-Se<sub>0.02</sub>-LDH, and Ni<sub>0.8</sub>Fe<sub>0.2</sub>-m/t-Se<sub>0.02</sub>-LDH

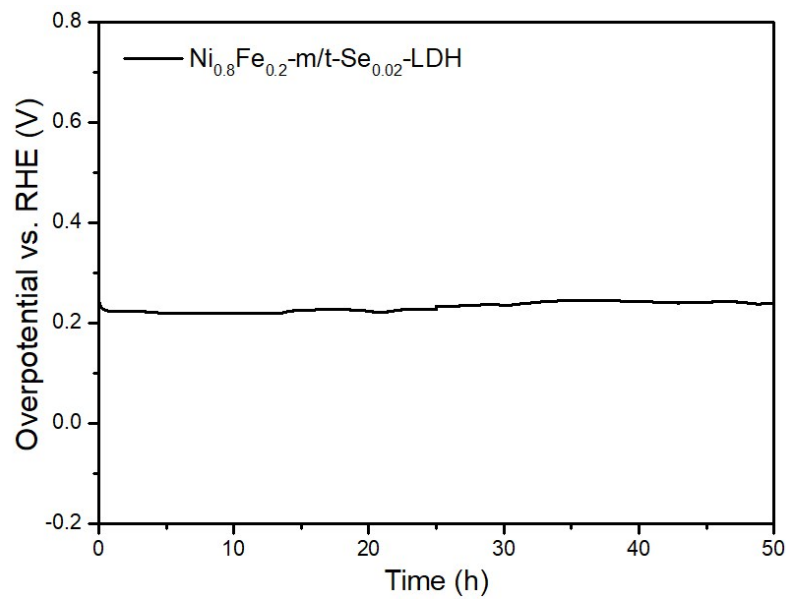


**Figure S16.** Chronopotentiometric curve for  $\text{Ni}_{0.8}\text{Fe}_{0.2}\text{-m/t-}\text{Se}_{0.02}\text{-LDH}$  in 1.0 M KOH electrolyte for 50 h.

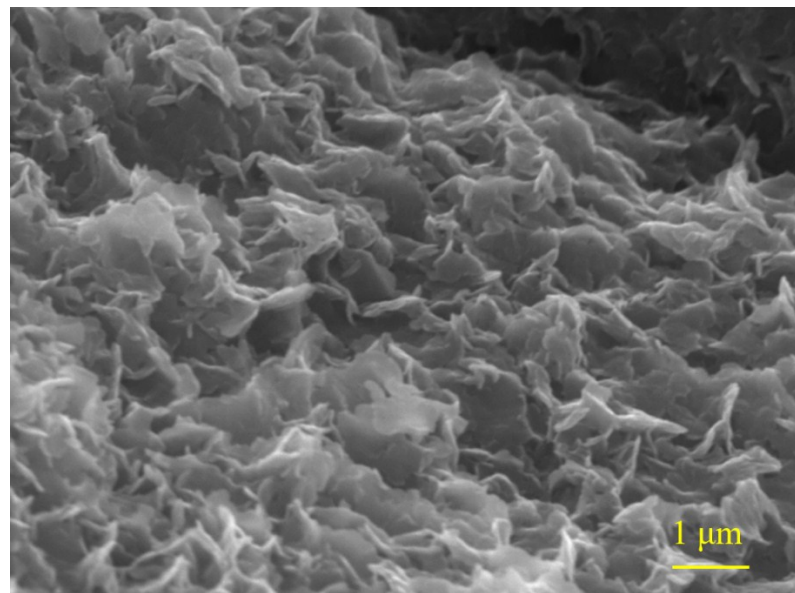


**Figure S17.** SEM image of  $\text{Ni}_{0.8}\text{Fe}_{0.2}\text{-m/t-}\text{Se}_{0.02}\text{-LDH}$  after OER measurement.

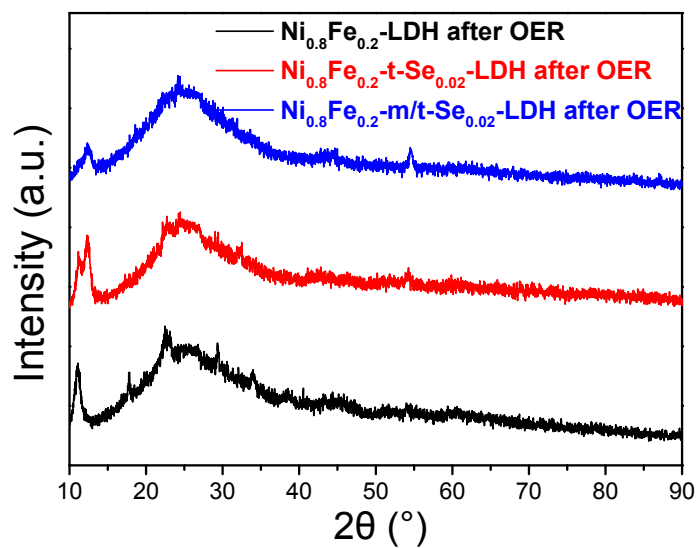


**Figure S18.** XRD patterns of the studied catalysts after OER measurement

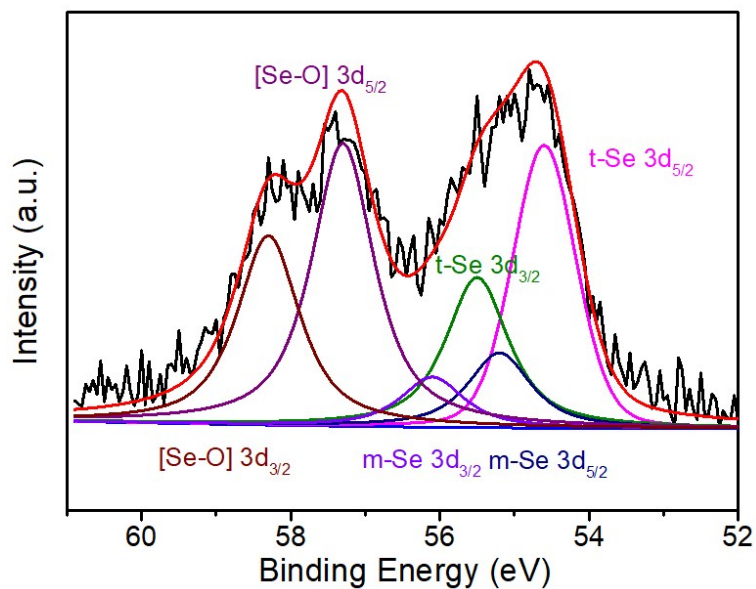


**Figure S19.** High-resolution Se 3d XPS spectrum of  $\text{Ni}_{0.8}\text{Fe}_{0.2}\text{-m/t-Se}_{0.22}\text{-LDH}$  after OER measurement



**Figure S20.** The photograph of electrochemical overall water splitting cell ( $\text{Ni}_{0.8}\text{Fe}_{0.2}\text{-m/t-Se}_{0.02}\text{-LDH//Pt/C}$ ).

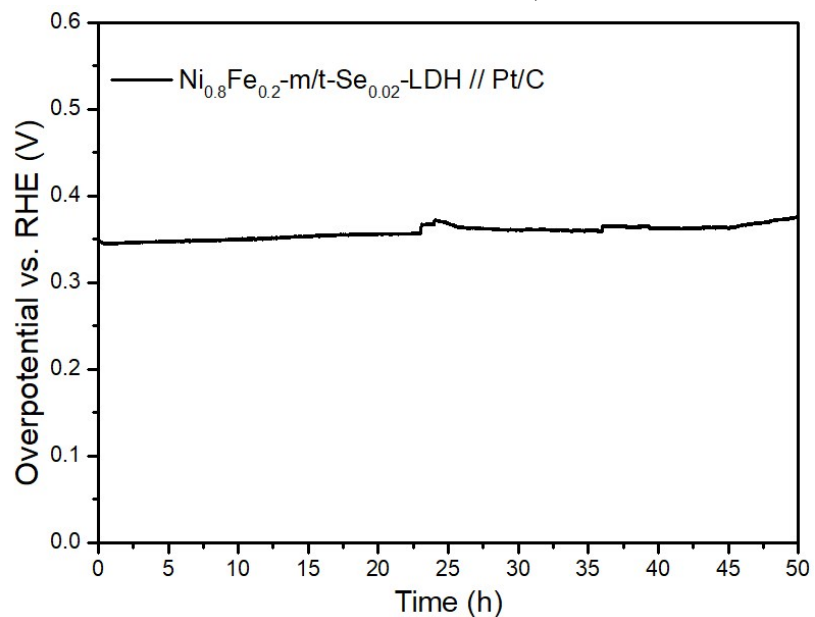


**Figure S21.** Overall water splitting polarization curves of  $\text{Ni}_{0.8}\text{Fe}_{0.2}\text{-m/t-Se}_{0.22}\text{-LDH//Pt}$  in 30 wt% KOH electrolyte for 50 h.

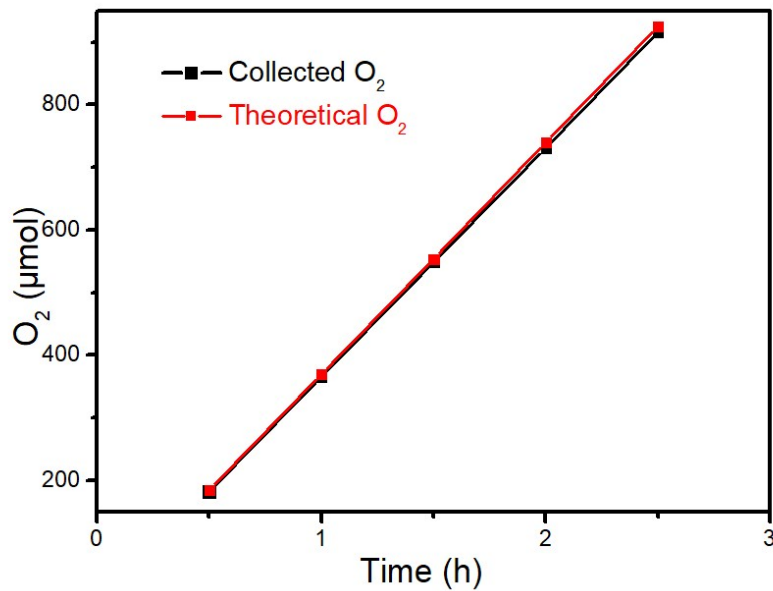


**Figure S22.** The amount of theoretically calculated (red line) and experimentally measured (black line) oxygen versus time for  $\text{Ni}_{0.8}\text{Fe}_{0.2}\text{-m/t-Se}_{0.22}\text{-LDH}$  in 1.0 M KOH electrolyte.

**Table S1.** Elemental compositions of the studied catalysts before and after OER measurements.

	Ni	Fe	O	Se	Fe/Ni ratio
$\text{Ni}_{0.8}\text{Fe}_{0.2}^{-\text{m/t}}\text{Se}_{0.02}\text{-LDH}$	35.18	9.08	54.78	0.96	0.258
$\text{Ni}_{0.8}\text{Fe}_{0.2}^{-\text{t}}\text{Se}_{0.02}\text{-LDH}$	35.26	9.23	54.56	0.95	0.262
$\text{Ni}_{0.8}\text{Fe}_{0.2}\text{-LDH}$	32	9.43	58.57	-	0.295
$\text{Ni}_{0.8}\text{Fe}_{0.2}^{-\text{m/t}}\text{Se}_{0.02}\text{-LDH after OER}$	30.94	8.07	60.09	0.9	0.261
$\text{Ni}_{0.8}\text{Fe}_{0.2}^{-\text{t}}\text{Se}_{0.02}\text{-LDH after OER}$	33.04	7.89	58.16	0.91	0.239
$\text{Ni}_{0.8}\text{Fe}_{0.2}\text{-LDH after OER}$	33.59	3.22	63.19	-	0.096